RSC Advances

PAPER

View Article Online
View Journal | View Issue

Cite this: *RSC Adv.*, 2025, **15**, 9594

Evaluation of the mechanical and chemical properties of bitumen fractionation *via* time efficient chromatography techniques

Brittany Hallmark-Haack, *[a] Joshua Middleton,[a] Ana Luiza Rodrigues,[b] Michael Forrester,[a] R. Christopher Williams[b] and Eric Cochran[a]

Received 27th December 2024
Accepted 12th March 2025

DOI: 10.1039/d4ra09045d

rsc.li/rsc-advances

Bitumen, a crucial component of asphalt pavements, exhibits complex chemical properties that influence its performance. Traditional methods for separating bitumen into saturate, aromatic, resin, and asphaltene (SARA) fractions often suffer from limitations such as low efficiency and insufficient sample recovery. Here, we present a novel approach using flash chromatography to address these challenges. Our automated technique offers rapid and efficient separation of bitumen into fractions, enabling comprehensive characterization. To identify the most suitable column for bitumen characterization, we tested four different commercial columns packed with various stationary phases. By analyzing the separated fractions using analytical chemistry techniques and rheology testing, we demonstrated that each column type exhibits unique separation capabilities. Among the tested columns, the C18 column proved to be particularly valuable for obtaining comprehensive insights into the overall molecular structure and properties of bitumen. This research contributes to a deeper understanding of bitumen's molecular structure and its potential for developing higher-performing and longer-lasting asphalt pavements.

1 Introduction

Bitumen, a complex hydrocarbon mixture derived from petroleum refining, is a crucial component of asphalt pavements.[1,2] Its performance, influenced by its chemical composition, is increasingly variable due to changes in crude oil feedstock and refining processes.[3–8] The growing demand for lighter petroleum products has led to the production of heavier bitumen residues, raising significant difficulties in ensuring consistent asphalt quality.[9–11] To address these issues, a deep understanding of bitumen's molecular structure is crucial. However, the complexity of bitumen, comprising thousands of unique molecular species, makes the isolation of individual molecules impractical, bordering on impossible.[8,12–14] While much is unknown about the exact nature of these molecules, they can be categorized into the saturate, aromatic, resin, and asphaltene (SARA) fractions, which classify the hydrocarbons by size and polarity.[15,16]

Traditional SARA fractionation methods, such as ASTM standards, rely on solvent precipitation and gravimetric analysis, often resulting in poor reproducibility, low sample recovery, and insufficient material for comprehensive characterization, usually limiting it to fraction composition.[17] While High-Performance Liquid Chromatography (HPLC), such as the method developed by Western Research Institute (WRI) under contract for the Federal Highway Administration,[12] offers improved resolution, the low volume of samples produced and the time-consuming process remains a challenge.[18]

This study introduces a novel approach using flash chromatography to address the limitations of traditional bitumen fractionation methods. By optimizing stationary phases and solvent gradients, we developed a rapid and efficient method for separating bitumen into its constituent fractions. Our automated technique offers significant improvements in terms of efficiency, reproducibility, and scalability, providing a reliable and effective alternative to existing methods. To identify the most suitable column for bitumen characterization, we tested four different commercial columns packed with various stationary phases. By analyzing the separated fractions using analytical chemistry techniques and rheology testing, we demonstrated that each column type exhibits unique separation capabilities. Among the tested columns, the C18 column proved to be particularly valuable for obtaining comprehensive insights into the overall molecular structure and properties of bitumen. This research contributes to a deeper understanding of bitumen and its potential for developing more sustainable and high-performance asphalt pavements.

[a]*Department of Chemical and Biological Engineering, Iowa State University, Ames, IA 50011, USA. E-mail: hallmark@iastate.edu*

[b]*Department of Civil, Construction and Environmental Engineering, Iowa State University, Ames, IA 50011, USA*

2 Background

SARA fractionation has been employed to simplify the complex bitumen matrix.[19] It categorizes bitumen into saturates, aromatics, resins, and asphaltenes based on polarity and molecular weight. This fractionation method is crucial for understanding the bitumen's chemical composition and predicting pavement performance, as it influences the asphalt's rheological behavior, susceptibility to cracking and deformation, and overall pavement performance.[20–22]

Saturates are the lightest and least polar family, followed by the aromatics. Saturates are straight and branched chain aliphatic hydrocarbons, whereas the eponymous aromatic fraction is rich cyclic (poly)aromatic molecules.[23] These nonpolar hydrocarbon fractions possess few to no heteroatoms.[24] In contrast, resins and asphaltenes exhibit increasing polarity, and they differentiate themselves according to strength and number of polar groups, molecular weight, and degree of aromaticity.[25] Resins are intermediate in properties, containing polar aromatic groups, non-polar paraffinic groups, and heteroatoms.[20,24,26] Asphaltenes are semi-solid particles and have the highest molecular weight and highest polarity of the four fractions. Asphaltenes, the most polar and heaviest fraction, are semi-solid particles composed of condensed aromatic structures of high molecular weight with aliphatic side chains and heteroatoms.[21,27] The general trends for each fraction are shown in Fig. 1 along with a representative molecule for each.

Each of the asphalt components impacts the material properties of the final asphalt pavement.[8,28] A higher presence of asphaltenes increases viscosity, while saturates/aromatics decrease ductility.[29] A higher ratio of polar fractions relates to higher stiffness and tensile strength,[2,20,27] but also higher crack propagation.[8,21,22] An excess of nonpolar molecules can cause permanent deformation, fatigue cracking in thick pavements, and moisture sensitivity. On the other hand, too many polar molecules are associated with brittleness, low-temperature cracking, and fatigue cracking in thin pavements.[25] The ratio of the SARA fractions in the bitumen is dependent on the crude oil source and processing procedures, varying from source to source and batch to batch.[3–6] Understanding the relationship between chemical composition and material properties is important for better prediction of asphalt pavement performance.

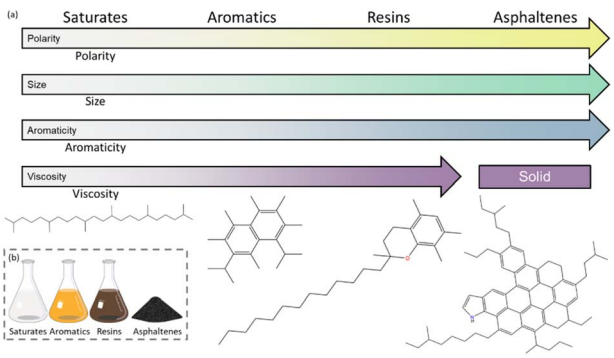

Fig. 1 (a) The trends in polarity, size, aromaticity, and viscosity are shown for the saturate, aromatic, resin, and asphaltene fractions of asphalt along with a representative molecule for each and (b) visualization of each fraction.

Bitumen has been extensively studied for the past 6 decades to improve its production and application, but the research has primarily focused on developing new methods for separating the bitumen rather than elucidating its mechanical and chemical properties.[30] The three main methods developed for SARA separation are (i) thin-layer chromatography (TLC), (ii) ASTM standards, and (iii) high-performance liquid chromatography (HPLC).

The first technique for SARA separation is thin-layer chromatography (TLC), typically combined with flame ionization detection (FID). A commercial technique called Iatroscan uses capillary TLC on silica or alumina rods to separate the fractions with a sequence of linear alkane, cyclohexane, toluene, and methylene chloride: methanol mixture. The rod is then slowly passed through FID to quantify the weight fraction of each hydrocarbon class.[31] The advantages to TLC-FID are that it is a fast and simple process that uses low amounts of solvents.[32] However, the drawbacks are that it has high error and does not effectively separate the asphaltenes. Furthermore, TLC-FID requires careful calibration to obtain a uniform FID response, and lighter fractions tend to evaporate.[15] Additionally, since the sample is burned to determine weight fractions, there is no material left for additional testing or analysis.[6]

The ASTM standard preparative procedures involve first diluting the asphalt in an *n*-alkane solvent. The saturates, aromatics, and resins, collectively known as the maltenes, dissolve in the n-alkane solvent.[33] The asphaltenes, however, do not dissolve and are removed by filtration.[15,34] The maltenes are then separated using column chromatography, with a calcined alumina column used to separate the components based on their polarity. Established in 1982, this standard was an improvement to the prior analysis of bitumen, but there are many drawbacks to it.[34]

This standard ASTM procedure requires a hand-packed column, which makes the process highly dependent on the skill and experience of the technician. Inconsistent packing can lead to flawed or non-reproducible results, requiring the experiment to be redone with a new sample. This wastes time, solvent, and sample. Even when an adequate run is obtained, the solvent use efficiency is often very poor, with 475 mL of solvent required to separate just 1 gram of bitumen.[15,34] The high amount of solvent used also necessitates significant time for solvent removal, further increasing experimental duration. Additionally, the entire SARA separation process takes 2.5 hours, excluding the time required for column packing and other preparatory work. Overall, the standard ASTM method is time-consuming, resource-intensive, and produces only minimal amounts of the separated fractions.[17]

Once the fractions are collected, further testing can be performed, including elemental analysis to determine the composition, differential scanning calorimetry or thermogravimetric analysis to characterize thermal behavior, infrared spectroscopy, and nuclear magnetic resonance spectroscopy to identify

chemical structures, gel permeation chromatography to determine molecular weight distribution and scanning electron microscopy for morphology.[3,35–37] However, the small sample sizes obtained using this technique limit the number of tests that can be performed and thereby restrict the amount of information that can be gathered about the asphalt binder.

Due to the aforementioned constraints of the preparative method, there was a shift towards automated chromatography. High-performance liquid chromatography offers several advantages, including the ability to control flow rate, regulate column temperature, provide precise solvent blends, detect fractions in real-time, and facilitate highly reproducible results thanks to its automated design. The use of HPLC for fractionating the maltenes allowed for even greater resolution of bitumen components with remarkable reproducibility.[38] The wide range of columns and solvents available allows for high customization of HPLC procedures.[17] However, the refractive index (RI) detection method can face calibration issues due to the extreme differences in response, and it lacks the flexibility to switch solvents.[17,31] Additionally, resins may irreversibly adsorb onto alumina and silica gel columns, necessitating backflushing to remove them and prevent column fouling.[15,18]

A method developed by Western Research Institute (WRI) under contract for the Federal Highway Administration brought about significant improvements to bitumen analysis. The WRI's SAR-AD is a fully automated high-performance liquid chromatography method that requires no prior asphaltene separation.[12] This system provides increased separation of bitumen into six distinct fractions compared to traditional chromatography, and it mitigates residual bitumen on the column, leading to more accurate compositional measurements. However, the HPLC method requires a 2 hour run time and can only separate 2 milligrams of sample per run. This HPLC technique is an improvement to the standard method with regards to fraction resolution, automation, and greater capacity for bitumen evaluation based on composition, but still only produces microscale amounts of each fraction.

Determining a way to link the composition of bitumen with its physical properties has long been a key goal in binder separation research, but this objective has remained largely elusive.[30] Existing methods like TLC-FID, column chromatography, and HPLC have significant limitations – TLC-FID is destructive, column chromatography is low throughput, and HPLC only separates 2 mg sample sizes. The complexity of the binder requires extensive separation to provide enough of each fraction for physical and rheological tests.[18] Furthermore, repeated use of the standard takes a copious amount of time, and the expense of the column stationary phase and solvents makes repetitions expensive. To advance bitumen analysis, a new technique is needed that can efficiently separate large amounts of sample in a timely and cost-effective manner.

A flash chromatography system meets these requirements and was used for the work documented in this paper. Flash chromatography offers numerous benefits, including reproducible and highly efficient separations due to its automated design.[6] The separations are quick, often completed within 45 minutes per run, and the pre-loaded columns eliminate the need for preparatory work. The flash chromatography industry has reported column loading capacities of up to 30%, leading to greater column and solvent efficiency compared to HPLC and significantly higher solvent efficiency than the gravimetric column method.

To evaluate reproducibility and efficiency, multiple separation runs were conducted, cumulatively fractionating over 10 grams of asphalt per column without fouling. Additionally, flash chromatography's automated design optimizes the elution conditions, reducing solvent consumption and minimizing waste compared to traditional methods. Its combination of high throughput, improved solvent efficiency, and reduced labor requirements reinforces its cost-effectiveness and suitability for large-scale bitumen fractionation in research and quality assurance/quality control (QA/QC) applications. Unlike HPLC and TLC, which are restricted to small sample sizes, flash chromatography enables the separation of multigram quantities of material in a single iteration, enabling the recovery of bitumen fractions in quantities suitable for detailed chemical and physical analyses.

For bitumen, it was found that the chosen experimental conditions, for example, the used solvents, different dimensions of the columns, and different materials for the mobile phase, affected the proportion of the bitumen fractions.[39] The selection of amine, C18, diol, and silica columns for flash chromatography was based on both technical and practical considerations. These columns effectively separate bitumen fractions according to their chemical affinities, as supported by previous studies.[40–42] Polar interactions (silica, amine, diol) enable separation based on polarity, and hydrophobic retention (C18) isolates nonpolar components. Additionally, hydrogen bonding (diol, amine) enhances selectivity, further confirming their effectiveness. From a practical perspective, these columns are readily available, cost-effective, and highly reusable, making them a scalable choice for large-scale applications. This ensures that the approach remains both feasible and sustainable for broader implementation.

3 Experimental plan

3.1 Materials

A performance grade XX-34 bitumen was provided by Flint Hills for use in all experiments. This study serves as an initial step in a larger body of work aimed at evaluating the applicability of flash chromatography across a broader range of bitumen types. While we focused on a single bitumen sample in this study to establish the methodology, future research will explore its effectiveness on different bitumen grades, sources, and polymer-modified binders. The following analytical-grade materials were purchased from Fisher Scientific and used as received: neutral alumina, dichloromethane, ethyl acetate, methanol, *n*-heptane, *n*-hexane, toluene, and trichloroethylene. The chromatography columns used in this study were SNAP Ultra C18 12 g, SNAP NH 28 g, and SNAP Ultra 10 g columns from Biotage, as well as Buchi Diol 12 g columns from Buchi. All columns were used as received without further modification.

3.2 Asphalthene separation

Asphaltenes were precipitated in n-alkane solvents to separate them from the maltenes. Approximately 50 g of bitumen at 70 °C was poured into a 1 L round bottom glass flask. Then, 500 mL of hexanes were added, and the solution was mechanically agitated and refluxed at 90 °C for 1 hour. Afterward, the heating mantle was turned off, and the solution was allowed to cool while still stirring. This process suspended the asphaltenes in hexanes and dissolved the maltenes. This process precipitated the asphaltenes, which were then removed by filtering the solution through a 25 μm filter paper. The asphaltenes were washed with *n*-hexane three times to ensure complete removal of the maltenes fraction. The isolated asphaltenes were then collected and dried under vacuum. The maltenes fraction was recovered by evaporating the *n*-hexane solvent from the filtered solution using a Collegiate BUCHI Rotavapor with a hot water bath.

3.3 ASTM standard

The ASTM D4124-09 standard procedure was followed to fractionate the maltenes into the traditional saturate, aromatic, and resin fractions.[34] A 1 g sample of maltenes was dissolved in 10 mL of *n*-heptane. A 70 cm long, 1.5 cm diameter column was packed with 110 g of calcined alumina, neutral. The column was carefully filled with *n*-heptane to prevent cracking of the alumina bed. The sample solution was slowly added to the top of the column, and excess solvent was removed until the sample was flush with the top of the column. Fractions were then collected by adding solvents according to the specifications in Table 1. The fractions were reclaimed by evaporating the solvents using a Collegiate BUCHI Rotavapor with a hot water bath.

3.4 Flash chromatography

Maltene fractionation was performed using a Biotage Isolera Spektra Systems flash chromatography system. An ultraviolet (UV) detector was employed for analyte detection at 285 nm. Distinct fractions were identified based on peaks observed in the detector output. Each elution required 18–20 column volumes (CV). The average sample mass loaded onto the column was 10–20% of the column packing mass. All columns were found to be reusable without deterioration for at least 50 consecutive trials. Maltenes were loaded onto the column by thinning with around 10 wt% toluene and injecting the mixture into the feed port. The mobile phase was configured for each column type using a combination of methanol, ethyl acetate, toluene, hexanes, and dichloromethane to provide a range of polarities. Solvent gradients were employed to provide a chemical potential gradient that maximized the separation between distinct fractions. The details for each method are shown in Fig. 3. Prior to initial elution, the columns were equilibrated with a 100% solution of the first solvent. Lastly, the solvent from each fraction was removed using a Collegiate BUCHI Rotavapor with a hot water bath, and the mass of the remaining asphaltic material was recorded. The retention factor k was calculated by dividing the time each fraction eluted from the column by the total elution time.

Table 1 Eluant solvent and eluate fractions used for the fractionation of maltenes into saturates, aromatics, and resins. Table copied from ASTM D4124-09 (ref. 34)

Eluant solvent	mL	Eluate fraction	mL
n-Heptane	150	Saturates	183
Toluene	33		
	67	Aromatics	142
Methanol/Toluene (50/50)	75		
Trichloroethylene	150	Resins	150

3.5 Elemental analysis

Elemental analysis was conducted on 2 to 3 mg samples loaded into aluminum capsules, with the addition of 5 to 8 mg of V_2O_5 from Sigma Aldrich. Triplicates were prepared for each sample. Elemental analysis results (% C, % H, % N, % S) were acquired using a PE 2100 Series II combustion analyzer (PerkinElmer Inc., Waltham, MA). The calibration standard used was cysteine. The expected precision and accuracy for each element was within ±0.3%. The combustion and reduction temperatures were both at 975 °C. All standards and reagents are from PerkinElmer and/or Elementar America's, Inc.

3.6 Gel permeation chromatography

Gel permeation chromatography was performed on 5 mg samples dissolved in 2 mL of tetrahydrofuran (THF) and filtered through a 0.45 μm filter. A Dionex/Thermo Scientific Ultimate 3000 Binary Semipreparative LC System (Sunnyvale, CA) equipped with two Agilent PLgel 3 μm 100 Å 300 × 7.5 mm columns, one Mesopore 300 × 7.5 mm column and a Diode Array Detector (DAD) was used. The mobile phase was THF at 1.0 mL min^{-1} and 25 °C. Polystyrene standards were purchased from Agilent (Agilent Technologies, Inc., Santa Clara, CA) and diluted with THF to 1 mg mL^{-1}. The wavelengths used for analysis were 254 nm, 263 nm, and 280 nm. The number average (M_n), weight average (M_w), and polydispersity ($Đ$) were calculated based on polystyrene standards.

3.7 Modulated differential scanning calorimetry

Sample masses of 5–15 mg were placed in Tzero aluminum hermetic pans. Modulated DSC measurements were performed using differential scanning calorimetry (TA Q2500). The samples were heated from −100 °C to 200 °C at a heating rate of 1.3 °C min^{-1}, with a modulation amplitude of 1.0 °C and modulation period of 60 s. The glass transition temperature (T_g) was obtained by using TA Instruments' Trios software.

3.8 Dynamic shear rheology and master curve construction

An Ares G2 (TA Instruments) equipped with an ACS-2 air chiller and 8 mm parallel plates with 1 mm gap was used to perform rheological measurements on the base binder and each fraction collected from the flash chromatography separations. Isochronal strain sweeps were performed to select the strain within the linear viscoelastic regime for each specimen. Isothermal frequency scans were performed from $\omega = 0.1$ to 100

rad^{-1} s on samples at temperatures ranging from −30 °C to 150 °C. Trios software from TA Instruments was used to construct master curves using time–temperature superposition. The Arrhenius equation was used to provide shift factors (a_T) for temperatures below the T_g, where a_0 and a_1 are the Arrhenius model parameters. For temperatures above the T_g, Williams–Landel–Ferry (WLF) equation was used to provide a_T, with C_1 and C_2 as the material constants.[7] T is the test temperature, and T_R is the reference temperature, which was chosen to be 50 °C for all master curves.

$$\log \alpha_T = a_0 + a_1\left(\frac{1}{T} - \frac{1}{T_R}\right)$$

$$\log a_T = -\frac{C_1(T - T_R)}{C_2 + T - T_R}$$

The master curves of complex modulus and phase angle were fitted using the Christensen–Anderson–Marasteanu (CAM) model. Equations are shown below, where G^* = complex modulus, G_g = glassy modulus, ω = frequency, ω_c = crossover frequency, R = rheological index/shape parameter, and δ = phase angle. Fig. 2 is a representation of each parameter fitted to a master curve. Microsoft solver was used to converge on values for G_g, ω_c, and R by minimizing the sum of squared errors between the measured and predicted values. Trios software was used to determine steady state viscosity (η_0) at low frequencies.

$$G^*(\omega) = G_g\left[1 + \left(\frac{\omega}{\omega_c}\right)^{\frac{\log 2}{R}}\right]^{-\frac{R}{\log 2}}$$

$$\delta(\omega) = \frac{90}{1 + \left(\frac{\omega}{\omega_c}\right)^{\frac{\log 2}{R}}}$$

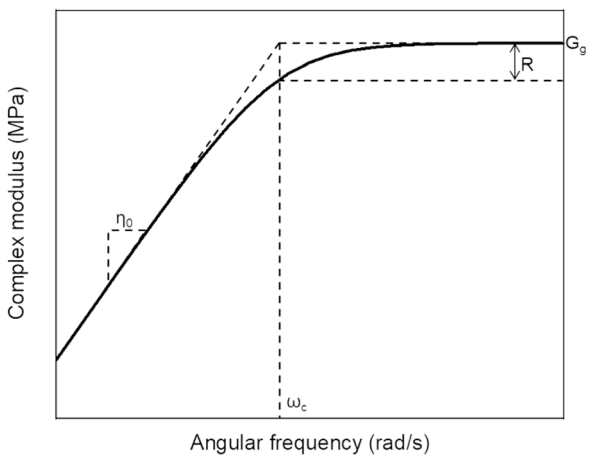

Fig. 2 CAM model parameters.

$$\mathrm{SSE} = \left(G' - G^*_{\mathrm{CAM}} \times \cos\delta_{\mathrm{CAM}}\right)^2 + \left(G'' - G^*_{\mathrm{CAM}} \times \sin\delta_{\mathrm{CAM}}\right)^2$$

Master curves were converted to a temperature ramp at explicit frequency of 10 rad s^{-1}. The temperature where $G^*/\sin\delta$ equals 1 was determined and recorded as the performance grade (PG) high failure temperature for unaged samples as indicated in ASTM D7175-23.[43]

4 Results and discussion

Flash chromatography is an automated technique that separates complex samples into distinct fractions based on the interaction between the solute and the stationary and mobile phases. The stationary phase contains functionalized silica beads, and as the mobile phase changes, solute molecules will either remain attached to the stationary phase or disperse into the mobile phase. Molecules that have a high affinity for the stationary phase have longer elution times than molecules with low affinity. The eluent leaving the column is monitored by a UV detector. Fig. 3 shows the schematic of the flash chromatography system used to separate maltenes of an asphalt binder. Four stationary phase columns were chosen for further investigation (amine, silica, C18, and diol).

Amine, silica, and diol columns are normal phase columns,[17] where the stationary phase is polar, and the solvents increase in polarity. The separation mechanism is adsorption, in which compounds are retained based on their affinity for the column. Nonpolar molecules spend the least amount of time in the column, while polar spend the most. Silica columns are preferred for flash chromatography due to their high stability, resolution, and reproducibility.[44] Amine columns have propyl amino functional groups bonded to high-purity silica, and diol columns are functionalized with 2-hydroxypropyl.

In contrast, C18 columns operate on a reverse-phase chromatography process, where the stationary phase is non-polar, and the mobile phases are polar solvents. For large and stretched molecules, the separation mechanism for reverse phase chromatography appears to be solute partitioning between the stationary phase and the solvent.[45,46] In this mechanism, the interaction between the solute molecules and the stationary phase is dependent on the amount of surface contact between the two, and therefore, solute retention increases with chain length.[45,47] This phenomenon is known as slalom chromatography, where separation follows a reverse size exclusion trend, with smaller molecules eluting first and larger molecules eluting later.[46]

The output signal *versus* mobile phase composition for each column is shown in Fig. 2b–d. The UV signal illustrates the distinct separation between fractions on each column, indicating the successful separation of individual fractions. The retention factor and weight fraction for each fraction can be found in Table 2, along with the rheology parameters, T_g, M_n, M_w, and $Đ$. Elemental analysis data is presented in Fig. 4. The T_g, size distribution, and elemental analysis data were collected

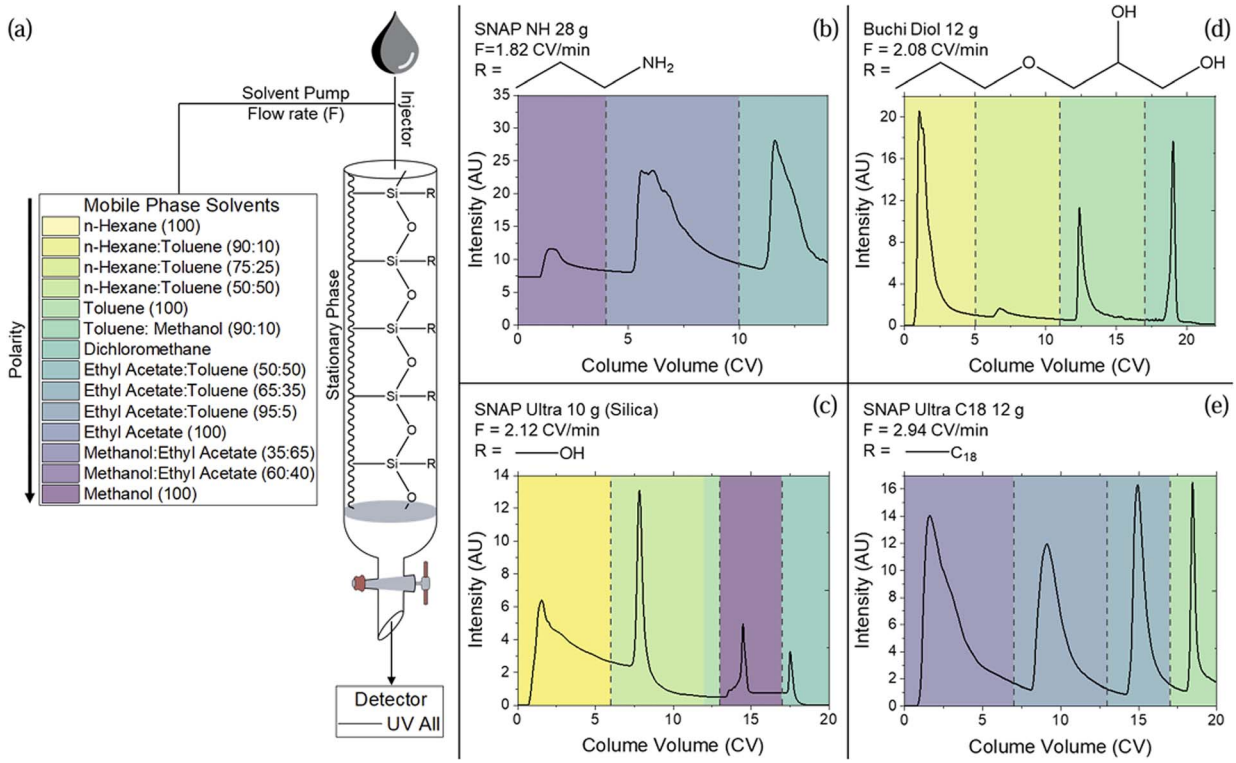

Fig. 3 (a) Flash chromatography schematic with mobile phase solvents, and output signal *vs.* mobile phase composition for (b) amine column, (c) silica column, (d) diol column, and (e) C18 column. Dashed vertical lines indicate cut points between fractions.

Table 2 XX-34 Bitumen fractionation data

Entry	Retention factor, k	w	High fail temp. (°C)	G_g[a] (MPa)	$\log(\eta_0)$ (Pa s)	R	MD Sc	T_g (°C)	M_n[b] (kDa)	M_w[b] (kDa)	$Đ$
Amine-1	0.100	0.16	26.8	756	7.75	1.13	0.81	−32.3	0.272	0.349	1.3
Amine-2	0.387	0.66	23.0	386	7.44	1.09	0.68	−37.8	0.401	0.833	2.1
Amine-3	0.787	0.18	104.5	761	1.67	6.12	2.46	82	0.789	4.140	5.2
Silica-1	0.090	0.63	13.8	1114	8.68	0.69	0.78	−40.8	0.347	0.985	2.8
Silica-2	0.400	0.23	78.7	109	4.46	4.16	1.12	31.3	0.637	2	3.1
Silica-3	0.725	0.11	68.7	92	4.65	3.58	1.06	58.4	0.758	3.21	4.3
Silica-4	0.880	0.04	120.5	24	−0.55	—	1.26	69.6	0.609	2.3	3.8
C18-1	0.135	0.48	18.6	615	8.05	0.86	0.69	−31.8	0.295	0.435	1.5
C18-2	0.470	0.36	34.2	673	7.29	1.64	1.23	−28.2	0.715	1.6	2.2
C18-3	0.775	0.12	161.4	279	−3.22	10.98	1.61	107	1.47	5.86	4.0
C18-4	0.930	0.04	—	247	−5.97	—	2.55	168	1.23	10.1	8.3
Diol-1	0.050	0.79	15.2	683	8.11	0.79	0.79	−35.1	0.367	0.881	2.4
Diol-2	0.314	0.04	25.9	753	8.51	0.51	0.87	−30.7	0.385	1.05	2.7
Diol-3	0.573	0.04	92.5	493	3.31	4.16	1.48	61	0.581	2.77	4.8
Diol-4	0.873	0.13	100.7	16	−0.30	6.19	2.03	74.5	1.08	4.86	4.5
Saturates		0.35						−56.2	0.327	0.479	1.5
Aromatics		0.45						−29.2	0.355	0.737	2.1
Resins		0.21						2.05	0.693	3.84	5.6
Asphaltenes		0.14						173	0.76	5.54	7.3
XX-34		1.000	58.2	1291	6.52	2.54	1.56	−28.5	0.504	2.93	5.8

[a] Not all samples reached glassy plateau. [b] Normalized to styrene.

for the preparative maltene fractionation, asphaltenes, and base bitumen for comparison. Rheology was not measured on the preparative maltene fractions due to the limited material collected nor on the asphaltenes due to their powdery nature.

To apply flash chromatography on a large scale as a routine method in a laboratory setting, it is important to use appropriately sized columns and optimize flow rates to increase throughput. Automating sample loading, fraction collection,

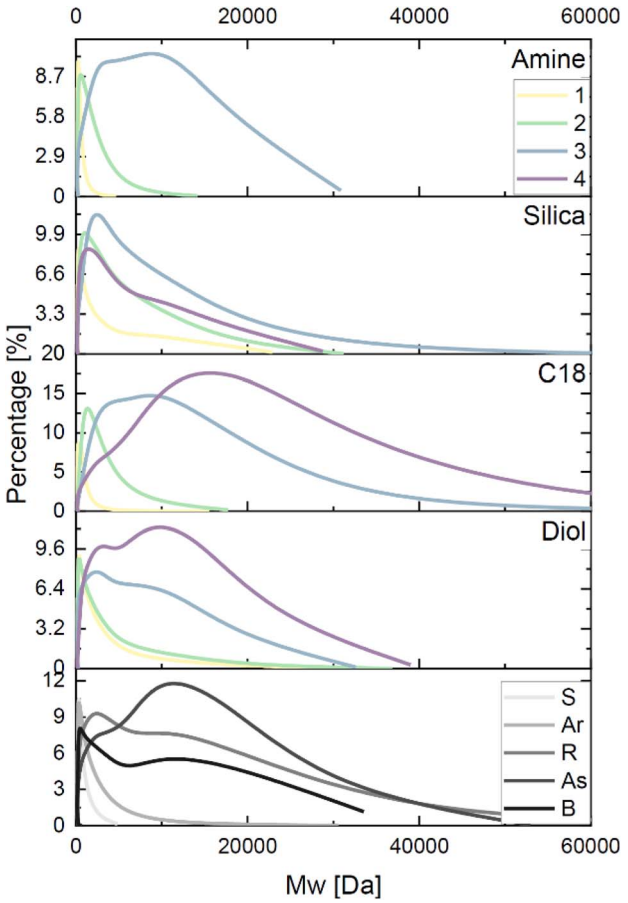

Fig. 4 GPC data for each of the four flash chromatography columns and the preparative maltene fractionation, where S = saturates, Ar = aromatics, R = resins, As = asphaltenes, and B = bitumen.

and solvent management ensures consistency and efficiency throughout the process. While solvent recycling is beyond the scope of this study, if flash chromatography were to become a standard method in a lab, a fractional distillation setup could be employed for solvent recovery, though further development may be needed depending on the solvents used. Based on our experience in this study, the flash chromatography method demands only about 10% of the solvent required for traditional SARA fractionation methods, significantly reducing solvent consumption. The cost of the necessary chromatography equipment for asphalt applications is approximately $30 000. This lower solvent demand improves cost-effectiveness and environmental impact, making it possible to perform basic return-on-investment calculations. Additionally, preventing column fouling through sample pretreatment and regular maintenance is essential for minimizing downtime and operational costs, ensuring reliable long-term performance.

Table 2 presents the high failure temperature and CAM model parameters for each sample. The high failure temperature is critical for assessing the asphalt binder's stiffness and elasticity under high service temperatures. It indicates the maximum average seven-day temperature that a pavement can withstand before failure. As the material transitions to a more solid-like state, the $G^*/\sin\delta$ value increases, corresponding to a higher performance grade. Four key parameters are calculated from the CAM model (Fig. 2): G_g, ω_c, R, and η_0. G_g, the limiting shear modulus, represents the material's behavior at very high frequencies or low temperatures and is indicative of the asphalt's elastic properties.[48] For some fractions, a glassy plateau was not achieved in the master curve construction, suggesting that these values may not be fully reflective of the true material behavior. Consequently, this parameter is minimally used for evaluating fractionation results. η_0, the viscous asymptote of the shear modulus, represents the material's viscous behavior at low frequencies or high temperatures and can provide insights into how the asphalt will perform under long-term loading conditions.[48] ω_c, the frequency at which the storage and loss moduli are equal, infers material hardness—higher values indicate softer material, while lower values suggest stiff, brittle behavior.[48–51] The R value, representing the difference between G_g and G^* at ω_c, is related to the material's relaxation spectrum and molecular weight distribution.[48,52] Furthermore, the R is a shape parameter that is linked to molecular weight.[53] As R increases, the master curve becomes flatter, indicating a more rigid, brittle material.[51,54,55]

The rheological analysis reveals distinct trends across the various fractions obtained from the different chromatographic methods. For the amine column, the first two fractions exhibit similar rheological properties, indicating relatively soft material. However, the last fraction contains stiffer and more brittle material, shown by increased high failure temperature, R and viscosity.

The silica column shows a similar pattern, with the first fraction containing very soft material and the last fraction being stiffer. The intermediate second and third fractions have comparable rheological characteristics, representing medium-stiffness material.

In the case of the C18 and diol columns, a clear trend emerges from the first to the last fraction: the high-temperature PG increases, G_g decreases, ω_c decreases, η_0 increases, and R increases. These changes collectively suggest that the later fractions obtained using these methods contain bulky, brittle, and stiff molecules, while the earlier fractions are relatively light, flexible, and soft.

T_g, the temperature at which the material transitions from a viscous, rubbery state to a hard, glassy state, is closely related to molecular weight and structure. Compounds with high molecular weight or aromatic rings exhibit less flexibility, and higher T_g, while low molecular weight, saturated molecules have lower T_g.[56,57] The preparative maltene separation method shows an increase in T_g from saturates to aromatics to resins, with asphaltenes having the highest T_g. This is consistent with the literature discussion of each asphalt fraction, where size and aromaticity increase from saturates to asphaltenes (Fig. 1). Additionally, this trend is also observed in the flash chromatography methods, with the silica, C18, and diol columns demonstrating an increase in T_g from the first to the last fraction. In the amine column, the first and second fractions have similar T_g, with an increase in the third fraction, indicating that the earlier fractions likely contain lower molecular weight,

linear molecules, while the later fractions contain higher molecular weight, cyclic structures. Furthermore, the presence of heteroatoms, such as nitrogen and sulfur, can decrease molecular flexibility and increase T_g, contributing to the slight increase in T_g observed in the initial flash chromatography fractions compared to the saturates cut (Fig. 5).

Thus, these tests demonstrate that each fraction's rheology and molecular weight distribution contain valuable information that, due to the output limitations of traditional tests, has not been fully explored. Fractions with lower molecular weight and higher flexibility improve low-temperature cracking resistance, while those with higher molecular weight and aromaticity enhance high-temperature rutting resistance and stiffness. The flash chromatography method's capability holds the potential to provide key information to design binders that are more resistant to aging and oxidation, tailoring solutions to address different climatic and traffic conditions, ultimately improving long-term pavement performance.

The gel permeation chromatograms in Fig. 4 reveal the molecular weight distributions of the flash chromatography and preparative method fractions. As shown in Table 2, M_n and M_w generally increase with elution time for all methods. However, the last fractions of the silica and C18 columns are exceptions to this trend, compares the gel permeation chromatograms for each of the flash chromatography and preparative method fractions.

The fourth fraction of the silica column has a lower M_n and M_w compared to the third fraction. This can be attributed to the elemental analysis (Fig. 5), which shows the third silica fraction has a significantly higher percentage of nitrogen and oxygen, and lower percentage of carbon, compared to the fourth fraction. The third and fourth fractions both contain very large molecules, but the large molecules containing nitrogen and oxygen are removed in the third fraction while the large molecules with lower polarity are removed in the fourth fraction. The large molecules with lower polarity are likely to be slightly smaller than those with heteroatoms, resulting in the size decrease.

The second exception is that the fourth fraction of the C18 column, which has a lower M_n but a higher M_w with a large dispersity index when compared to the third fraction. As discussed previously, the separation mechanism of the C18 column is dependent on the molecular size and contact area between the molecules and the stationary phase. This wide distribution of molecular sizes in the fourth fraction could be attributed to the structure of the molecules. As shown in Fig. 5, the fourth fraction of the C18 column has the lowest H/C ratio of any fraction, thus it is likely to contain the highest ratio of aromatic rings. The presence of aromatic structures likely causes higher retention between the molecule and stationary phase, which would cause the higher aromatic moieties to elute later along with the extremely high molecular weight compounds, resulting in a large M_w but similar M_n. These aromatic structures also contribute to the rigidity of the material, as shown in the particularly brittle characterization derived from the rheology parameters and the exceptionally high T_g. Overall, the size separation of the C18 column is extremely successful. It has the widest distribution of M_n and M_w of any of the separation methods: the first fraction is among the lowest M_n, while the third fraction is the highest M_n, and the fourth fraction is the highest M_w. This column has the most efficient separation based on the size compared to the other flash chromatography columns.

Importantly, all the flash chromatography methods produce fractions with an average M_n higher than the preparative method's resin fraction. In Fig. 4, the resin has a broad

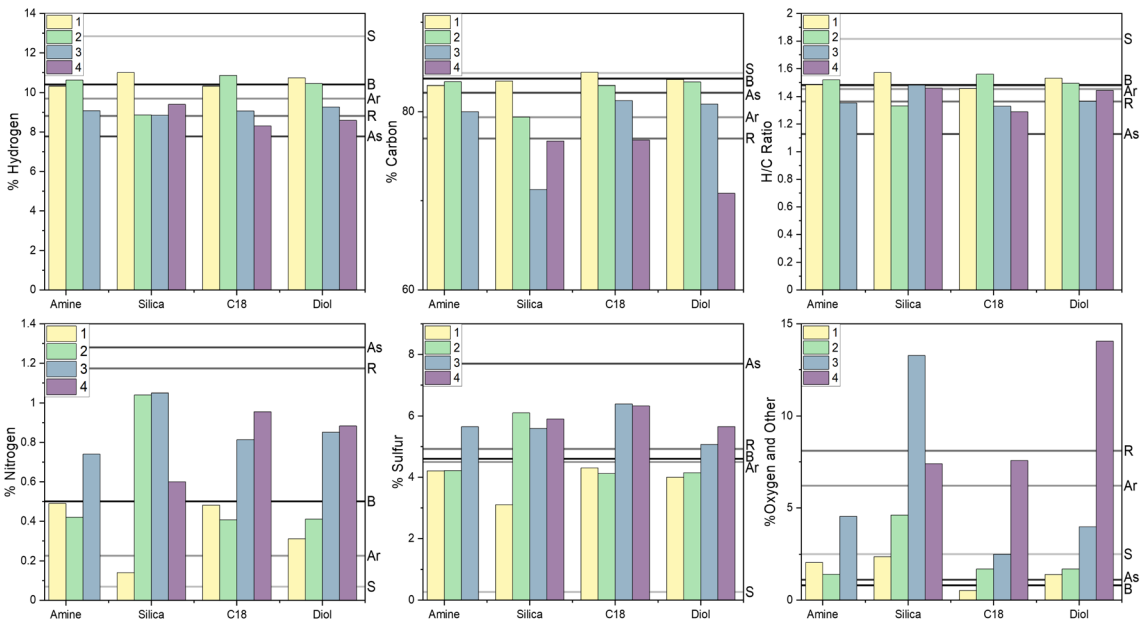

Fig. 5 Elemental analysis data for each column. Horizontal bars designate the preparative maltene fractionation values, where S = saturates, Ar = aromatics, R = resins, As = asphaltenes, B = XX-34 bitumen.

distribution with two peaks, and the dispersity index is 5.6, demonstrating that the resin fraction contains a wide range of molecular weight compounds hidden by the calculated values. Except for C18-4, the later fractions of all the flash chromatography methods have a lower dispersity index than the resins cut. Likewise, two of the methods contain a fraction where the average M_n is lower than the saturates cut, and the earlier fractions have similar or lower dispersity indexes than the saturates cut. Collectively, the flash chromatography methods have a wider range of reported sizes between fractions with a narrower distribution for each cut. This demonstrate the superior ability of flash chromatography to separate asphalt into distinct molecular weight fractions than the aforementioned SARA method.

Furthermore, both the C18 and diol methods have fractions with M_n larger than the asphaltene cut. Most literature designates the asphaltenes as the largest molecular class of asphalt fractions,[21,27] but the presence of these large fractions in the flash chromatography samples suggests that higher molecular weight compounds are present in the maltene fraction of asphalt – and that another factor is more dominant than size in separating the soluble maltenes and insoluble asphaltenes.

In the elemental analysis, the composition of hydrogen, carbon, nitrogen, and sulfur are evaluated, and all other elements are lumped together in one category (Fig. 5). For asphalt, this would be elements such as oxygen with trace amounts of metals such as iron or nickel. Since the amount of metals is negligible,[2] this category can be mostly attributed to oxygen, and is designated as % O^+.

The preparative method of maltene separation exhibits a clear trend in elemental analysis. Hydrogen and carbon content, along with the H/C ratio, decreases from saturates to aromatics to resins, while heteroatom content follows an inverse trend. The H/C ratio provides insight into molecular structure—higher values correspond to hydrogen-rich, branched, and linear aliphatic molecules, whereas lower values indicate a greater presence of aromatic rings and heteroatoms.[58,59] These findings align with literature,[2,60,61] where saturates are mostly aliphatic branched molecules, and resins contain more cyclic structures with heteroatoms (Fig. 1).

Like the preparative method, the flash chromatography fractions generally show a decrease in hydrogen and carbon content and H/C ratio with an increase in heteroatoms from the first to the last fraction. This confirms that early-eluting fractions are predominantly branched-chain aliphatics, while later fractions contain more cyclic molecules with heteroatoms. Notably, the third and fourth C18 fractions, as well as the second silica and third amine fractions, exhibit lower H/C ratios than the preparative resins cut, suggesting that these columns effectively separate aromatic structures.

The increased nitrogen, oxygen, and sulfur content in later fractions contributes to their higher polarity, as these electronegative elements form highly polar functional groups. These groups engage in electrostatic interactions, van der Waals forces, and hydrogen bonding, further influencing the fractionation behavior.[60] Additionally, each flash chromatography fraction contains higher nitrogen and sulfur levels than the saturates fraction, suggesting that this method efficiently isolates a greater proportion of small molecules with heteroatoms than previously recognized. This is consistent with the slightly elevated T_g values observed in the first flash chromatography fractions compared to the saturates cut (Table 2), indicating differences in molecular composition and interactions. Importantly, this result highlights that each chromatographic column separates the binder uniquely, both relative to one another and in comparison to traditional SARA fractionation.

The % O^+ category is particularly informative in assessing asphalt durability, as oxygen is known to accelerate aging, stiffening, and premature cracking.[62] Among the tested columns, diol and silica columns demonstrated exceptional efficiency in separating oxygen-containing compounds. This suggests their potential as predictors for problematic binders, as binders with a higher concentration of oxygenated species may be more susceptible to oxidative degradation.

Lastly, asphaltenes are considered to have the largest quantity of heteroatoms of the asphalt fractions.[2] While this is true for nitrogen and sulfur, asphaltenes have the lowest oxygen content. This demonstrates that a main factor behind the insolubility of asphaltenes is most likely due to the nitrogen and sulfur content rather than molecular size.

The flash chromatography method provides a more detailed molecular separation than conventional SARA fractionation, particularly in isolating heteroatom-rich fractions. This enhanced resolution could be valuable for asphalt formulation optimization, allowing for targeted modification strategies, such as the use of anti-aging additives or rejuvenators, to improve binder longevity. However, further studies are needed to correlate this information with asphalt performance, particularly in terms of aging, durability, and modification strategies.

5 Conclusions

This study introduces a novel approach using flash chromatography to address the limitations of traditional bitumen fractionation methods. By optimizing stationary phases and solvent gradients, we developed a rapid and efficient method for separating bitumen into its constituent fractions. Our automated technique offers significant improvements in terms of efficiency, reproducibility, and scalability, providing a reliable and effective alternative to existing methods.

By analyzing the separated fractions using analytical chemistry techniques and rheology testing, we demonstrated that each column type exhibits unique separation capabilities, as following:

– Amine column: Useful for simple separation of bitumen into soft and hard material.

– Silica column: Highly efficient at isolating oxygen-containing compounds.

– Diol column: Excels at separating components based on polarity and size.

– C18 column: Exceptional ability to separate based on molecular size, offering a wide range of fractions. The most evenly distributed weight fractions, making it the most

beneficial for obtaining insights into overall bitumen characterization.

This study discovered that the separation of asphaltenes from maltenes using n-alkane solvents is not solely determined by molecular size. Instead, the high nitrogen and sulfur content of asphaltenes plays a significant role in their insolubility. Additionally, flash chromatography has been shown to be more effective than traditional methods in separating bitumen into distinct molecular weight fractions, revealing the presence of smaller molecules containing heteroatoms that were previously overlooked.

Looking forward, future studies should aim to expand the use of flash chromatography to a broader range of bitumen samples, including recycled asphalt binders and polymer-modified binders. These materials are critical for the sustainability and performance of asphalt, and it is essential to investigate how flash chromatography can be applied to these more complex binders, which may pose challenges for separation. A comparative evaluation of flash chromatography against conventional methods will be important to confirm its reliability and precision when applied to these materials.

Understanding the chemical composition and key properties, such as the rheology of the different fractions, will provide valuable insights into the binder's behavior, enabling more effective formulation practices. This understanding could ultimately lead to improved pavement performance and more sustainable asphalt production methods. Large-scale implementation of flash chromatography, combined with these advancements, has the potential to foster more effective, environmentally friendly practices in asphalt production, enhancing the durability and sustainability of roadways.

Data availability

All data supporting this article have been provided within the main content of this manuscript. No additional data are available outside of this publication.

Author contributions

B. Hallmark-Haack: conceptualization, methodology, data curation, formal analysis, investigation, writing—original draft, writing—review and editing. J. Middleton: methodology, investigation, writing—review and editing. A. Rodrigues: investigation, writing—original draft, writing—review and editing. M. Forrester: conceptualization. R. C. Williams: conceptualization, funding acquisition. E. Cochran: conceptualization, funding acquisition, writing—review and editing.

Conflicts of interest

There are no conflicts to declare.

Acknowledgements

The authors would like to thank Lusi A and Moham Ed Abdur Razzaq for assistance pertaining to the Dionex/Thermo Scientific Ultimate 3000 Binary Semipreparative LC System. Purchase of the PerkinElmer 2100 Series II CHN/S analyzer used to obtain results included in this publication was supported in part by the National Science Foundation under Grant No. DBI 9413969. Any opinions, findings, and conclusions or recommendations expressed in this material are those of the author(s) and do not necessarily reflect the views of the National Science Foundation. The authors would also like to thank ISU Chemical Instrumentation Facility staff members Sara Cady and Kaitlyn Bennet for training and assistance pertaining to the PE 2100 CHN/S elemental analysis results included in this publication. Finally, the authors would like to thank Emily Smith and Ashley Marker for their assistance in laboratory work.

References

1 S. Li, J. Wu, Y. Wang, Y. Li, W. Zhang, Y. Zhang, K. He, C. Cai, G. Bian, H. Wang, Y. Ji and Q. Shi, *Fuel*, 2023, **335**, 127049.
2 R. N. Hunter, A. Self and J. Read, *The Shell Bitumen Handbook*, ICE Publishing, 6th edn, 2015.
3 C. Zhang, T. Xu, H. Shi and L. Wang, *J. Therm. Anal. Calorim.*, 2015, **122**, 241–249.
4 J. Peralta, L. Hilliou, H. M. R. D. Silva, A. Machado and R. C. Williams, *Rheol. Acta*, 2014, **53**, 143–157.
5 B. F. Law, Characterization of Laboratory Simulated Road Paving-like Asphalt by High Performance Liquid Chromatography and Gas Chromatography-Mass Spectrometry, Master of Science, West Virginia University, Morgantown, West Virginia, 2006.
6 L. Raki, J.-F. Masson and P. Collins, *Energy Fuels*, 2000, **14**, 160–163.
7 D. Yu, Y. Gu and X. Yu, *Fuel*, 2020, **265**, 116953.
8 S. Sultana and A. Bhasin, *Constr. Build. Mater.*, 2014, **72**, 293–300.
9 L. Cui, H. Chen, J. Xu, M. Ren and F. Cao, *Fuel*, 2020, **265**, 117002.
10 J. J. Adams, M. D. Elwardany, J.-P. Planche, R. B. Boysen and J. F. Rovani, *Energy Fuels*, 2019, **33**, 2680–2698.
11 J. S. Youtcheff and D. R. Jones, *Guidelines for Asphalt Refiners and Suppliers, SHRP Report A-686*, National Research Council, Washington, DC, 1994.
12 P. G. Redelius, *Fuel*, 2000, **79**, 27–35.
13 F. Rovasi Adolfo, P. Cícero do Nascimento, D. Bohrer, C. Viana, L. Machado de Carvalho, M. C. Coutinho Cravo and L. Nascimento, *Fuel*, 2020, **277**, 118098.
14 L. W. Corbett, *Anal. Chem.*, 1969, **41**, 576–579.
15 H. Bisht, M. Reddy, M. Malvanker, R. C. Patil, A. Gupta, B. Hazarika and A. K. Das, *Energy Fuels*, 2013, **27**, 3006–3013.
16 S. Mangiafico, H. di Benedetto, C. Sauzéat, F. Olard, S. Pouget and L. Planque, *Mater. Des.*, 2016, **111**, 126–139.
17 A. Karevan, M. Zirrahi and H. Hassanzadeh, *ACS Omega*, 2022, **7**, 18897–18903.
18 M. Boduszyński, B. R. Chadha and H. Pineles, *Fuel*, 1977, **56**, 145–148.
19 M. Santos, A. Vetere, A. Wisniewski, M. Eberlin and M. Schrader, *Energy Fuels*, 2020, **34**, 16006–16013.
20 L. Oyekunle, *IFP*, 2006, **61**, 433–441.

21 E. J. F. Peralta, Master's thesis, Universidade do Minho, 2009.
22 T. Wang, J. Wang, X. Hou and F. Xiao, *Road Mater. Pavement Des.*, 2021, **22**, 539–556.
23 J. Wang, T. Wang, X. Hou and F. Xiao, *Fuel*, 2019, **238**, 320–330.
24 G. Xu and H. Wang, *Fuel*, 2017, **188**, 1–10.
25 D. R. Jones, Understanding How the Origin and Composition of Paving-Grade Asphalt Cements Affect Their Performance, *SHRP Asphalt Research Program Technical Memorandum #4*, 1992.
26 L. Carbognani, M. F. Gonzalez and P. Pereira-Almao, *Energy Fuels*, 2007, **21**, 1631–1639.
27 K. J. Leontaritis and G. A. Mansoori, *J. Pet. Sci. Eng.*, 1989, **2**, 1–12.
28 D. D. Li and M. L. Greenfield, *Fuel*, 2014, **115**, 347–356.
29 O. Sirin, D. K. Paul and E. Kassem, *Adv. Civ. Eng.*, 2018, **2018**, DOI: **10.1155/2018/3428961**.
30 G. Li and Y. Tan, *Fuel*, 2022, **308**, 122037.
31 R. B. Boysen and J. F. Schabron, *Energy Fuels*, 2013, **27**, 4654–4661.
32 M. Makowska and T. Pellinen, *J. Traffic Transp. Eng., Engl. Ed.*, 2021, **8**, 453–466.
33 D. L. Mitchell and J. G. Speight, *Fuel*, 1973, **52**, 149–152.
34 ASTM International, *Annual Book of ASTM Standards*, ASTM International, West Conshohocken, PA, 2018.
35 J. Huang, *Pet. Sci. Technol.*, 2010, **28**, 618–624.
36 Y. Ding, B. Huang and X. Shu, *Fuel*, 2018, **227**, 300–306.
37 S. W. Bishara and E. Wilkins, *Transp. Res. Rec.*, 1989, **1228**, 183–190.
38 J. R. Woods, J. Kung, D. Kingston, L. S. Kotlyar, B. D. Sparks and T. W. McCracken, *Oil Gas Sci. Technol.*, 2008, **63**, 151–163.
39 M. Porto, P. Caputo, V. Loise, S. Eskandarsefat, B. Teltayev and C. Rossi, *Appl. Sci.*, 2019, **9**, 742.
40 A. Karevan, M. Zirrahi and H. Hassanzadeh, *ACS Omega*, 2022, **7**, 18897–18903.
41 K. Schwettmann, P. Höhne and D. Stephan, *Mater. Struct.*, 2022, **55**, 242.
42 G. Šebor, J. Blažek and M. Nemer, *J. Chromatogr. A*, 1999, **847**, 323–330.
43 ASTM International, *Annual Book of ASTM Standards*, ASTM International, West Conshohocken, PA, 2023.
44 D. Wallace, D. Henry, K. Pongar and D. Zimmerman, *Fuel*, 1987, **66**, 44–50.
45 K. B. Sentell and J. G. Dorsey, *Anal. Chem.*, 1989, **61**, 930–934.
46 E. Uliyanchenko, *Anal. Bioanal. Chem.*, 2014, **406**, 6087–6094.
47 A. Vailaya and C. Horváth, *J. Chromatogr. A*, 1998, **829**, 1–27.
48 D. A. Anderson, *Binder Characterization and Evaluation, Physical Characterization; Strategic Highway Research Program*, National Research Council, Washington, DC, 1994, vol. 3.
49 E. Santagata, O. Baglieri, L. Tsantilis and D. Dalmazzo, *Procedia Soc. Behav. Sci.*, 2012, **53**, 546–555.
50 D. Mensching, N. Gibson, A. Andriescu, G. Rowe and J. Sias, *International Society for Asphalt Pavements Symposium and 53rd Petersen Asphalt Research Conference 2016*, 2016.
51 N. I. M. Yusoff, F. M. Jakarni, V. H. Nguyen, M. R. Hainin and G. D. Airey, *Constr. Build. Mater.*, 2013, **40**, 174–188.
52 M. Cholewinska, M. Iwanski and G. Mazurek, *Baltic J. Road Bridge Eng.*, 2018, **13**, 34.
53 J. C. Petersen, R. E. Robertson, J. F. Branthaver, P. M. Harnsberger, J. J. Duvall, S. S. Kim, D. A. Anderson, D. W. Christiansen and H. U. Bahia, *Binder Characterization and Evaluation*, DC, 1994.
54 L. F. M. Leite, P. H. Osmari and F. T. S. Aragão, *Constr. Build. Mater.*, 2022, **338**, 127549.
55 M. Ling, X. Luo, F. Gu and R. L. Lytton, *Constr. Build. Mater.*, 2017, **157**, 943–951.
56 J.-F. Masson, G. M. Polomark and P. Collins, *Energy Fuels*, 2002, **16**, 470–476.
57 P. Kriz, J. Stastna and L. Zanzotto, *Road Mater. Pavement Des.*, 2008, **9**(sup1), 37–65.
58 X. Xiao, Z. Chen and B. Chen, *Sci. Rep.*, 2016, **6**, 22644.
59 L. Yue, G. Li, G. He, Y. Guo, L. Xu and W. Fang, *Chem. Eng. J.*, 2016, **283**, 1216–1223.
60 S. Werkovits, M. Bacher, J. Theiner, T. Rosenau and H. Grothe, *Constr. Build. Mater.*, 2022, **352**, 128992.
61 M. Guo, M. Liang, Y. Fu, *et al.*, *Mater. Struct.*, 2021, **54**, 1–8.
62 L. Ma, A. Varveri, R. Jing and S. Erkens, *Constr. Build. Mater.*, 2021, **283**, 122632.